

## Photoelectric Effect and Planck's Constant in the Introductory Laboratory

Harry H. Hall and Richard P. Tuttle

Citation: *American Journal of Physics* **39**, 50 (1971); doi: 10.1119/1.1986055

View online: <http://dx.doi.org/10.1119/1.1986055>

View Table of Contents: <http://scitation.aip.org/content/aapt/journal/ajp/39/1?ver=pdfcov>

Published by the American Association of Physics Teachers

### Articles you may be interested in

[Improved student laboratory on the measurement of Planck's constant using the photoelectric effect](#)

*Am. J. Phys.* **56**, 86 (1988); 10.1119/1.15387

[A correction to the photoelectric current in the Planck's constant experiment](#)

*Phys. Teach.* **23**, 98 (1985); 10.1119/1.2341733

[A New Amplifier for the Photoelectric Effect and Planck's Constant Experiment](#)

*Am. J. Phys.* **39**, 1542 (1971); 10.1119/1.1976716

[APPARATUS FOR TEACHING PHYSICS: Inexpensive Apparatus for Studying the Photoelectric Effect and Measuring Planck's Constant](#)

*Phys. Teach.* **1**, 183 (1963); 10.1119/1.2350641

[Two Elementary Experiments to Demonstrate the Photoelectric Law and Measure the Planck Constant](#)

*Am. J. Phys.* **14**, 245 (1946); 10.1119/1.1990826



American Association of **Physics Teachers**

Explore the **AAPT Career Center** –  
access **hundreds of physics education and other STEM teaching jobs** at two-year and four-year colleges and universities.

<http://jobs.aapt.org>



# Photoelectric Effect and Planck's Constant in the Introductory Laboratory

HARRY H. HALL  
RICHARD P. TUTTLE\*

Department of Physics  
University of New Hampshire  
Durham, New Hampshire 03824

(Received 2 March 1970; revised 12 August 1970)

*This paper describes another approach to the photoelectric measurement of  $h/e$  which is practicable for the introductory laboratory. The method owes its success to a new way of minimizing photoemission by the anode. A common vacuum photocell (1P39) and slit replace the eyepiece and cross hairs of a student grating spectrometer, illuminated by an ac mercury arc. If the cell is favorably oriented to the incident light, photoemission by the anode at high cathode retarding potential (6 V) can be reduced to less than 0.4% of the maximum photocurrent with zero retarding potential at the 3650-Å line. The 120-Hz component is amplified and rectified for presentation on a 100  $\mu$ A dc meter. The maximum gain is sufficient to indicate full scale for a photocurrent of  $10^{-11}$  A. Stopping potentials for six lines between 3650 and 5770 Å are determined by plotting the square root of the photocurrent against retarding potential and by extending the straight portions of these plots to the axis. The slope of a straight line drawn through the stopping potentials, plotted against photon frequency, comes close to the accepted value of  $h/e$ . Perhaps the most instructive aspect of this experiment is the experience with electron and photon energies. The student observes directly that electrons ejected by uv photons are much harder to stop than those ejected by photons of yellow light.*

## INTRODUCTION

The classical determination of Planck's constant by means of the photoelectric effect demands the utmost refinement of dc measuring technique<sup>1</sup> and is hardly suited to the introductory laboratory. Now, with modern electronics, this fundamental experiment of quantum physics is becoming a regular part of this laboratory. While a number of approaches have been made,<sup>2-5</sup>

this paper describes yet another which has some new features of its own.

Einstein's photoelectric equation states that the KE of the most energetic photoelectrons equals the photon energy  $h\nu$  less the work  $e\phi$  to remove an electron through the surface of the cathode. If an opposing stopping potential  $V_s$  is applied, just sufficient to prevent these electrons from reaching the anode, then their KE is equal to  $eV_s$ . Dividing Einstein's equation by  $e$  then gives

$$V_s = (h/e)\nu - \phi.$$

The slope of the straight line plot of  $V_s$  against photon frequency should equal  $h/e$ . Because of contact potential and surface effects which are hard to measure, the work function  $\phi$  cannot be reliably determined by this means.

The principal experimental difficulty seems to lie in determining  $V_s$  in the face of certain masking effects. The largest of these is the emission of an opposing photocurrent by the anode, which rises with increasing retarding potential and ultimately overbalances and reverses the total photocurrent. At this apparent cutoff, the anode current is merely equal and opposite to the cathode current, and the corresponding magnitude of the retarding potential bears no direct relation to  $V_s$ . In more elaborate attempts to measure  $h/e$  by this method, every precaution is taken to eliminate anode emission by the design of special photocells. The cost of these cells is high, however, and is apt to exceed the resources of the introductory laboratory.<sup>6</sup> One photocell of moderate cost has a loop of platinum wire as an anode, which can be heated to evaporate any photosensitive material which may have migrated to it. Experience has shown that this procedure must be repeated before each determination of  $V_s$  to obtain reliable results.<sup>2,5</sup> While working with the 1P39, an inexpensive vacuum photocell, we have discovered that anode emission can be greatly reduced by suitably orienting the cell to the incident light.

To avoid the need for an ultrasensitive electrometer as detector, an ac-powered mercury arc is used as a source, and the 120-Hz component of the photocurrent is amplified by ac methods, so that its rectified output can be shown on a dc meter. This also avoids difficulties with zero drift, which can be critically important near current cutoff.

## DESCRIPTION OF THE EXPERIMENT

Light from the principal bright lines of an ac powered mercury arc, formed in a grating spectrometer, illuminates the cathode of a 1P39 photocell, which has been oriented to minimize anode emission. A capacitance coupled amplifier amplifies the 120-Hz component of the photocurrent, which is rectified and presented on a dc meter. A retarding potential applied to the photocathode is increased until the photocurrent is extinguished. Plotting the square root of the photocurrent against retarding potential and extending the straight part to zero photocurrent determines  $V_s$ , the "stopping potential" (actual stopping potential+contact potential).<sup>7,8</sup> A typical plot of  $V_s$  against photon frequency for six lines between 3650 and 5770 Å yields a fairly straight line whose slope is close to the accepted value of  $h/e$  (see Fig. 1).

## REDUCTION OF ANODE EMISSION BY PHOTOCELL ORIENTATION

The cathode of the 1P39 is semicylindrical, with the photosensitive coating on its inner surface. The anode is a thin rod supported on the axis of the cathode. If light of the shortest wavelength to be used (3650 Å) falls on the inner side of the cathode in the normal manner, and the cell is gradually turned about its major axis while the retarding potential is varied above and below current cutoff, the anode current abruptly ceases as the cathode edge begins to shadow the anode, as in Fig. 2. Before rectification, the ac cathode and anode currents are in opposite phase. After rectification, they are both positive, but the former decreases with increasing retarding potential, while the latter increases, so that the anode current can be separately identified. If the cell is turned slowly back again, the anode current suddenly reappears, but just before this the cathode current usually rises rapidly. The

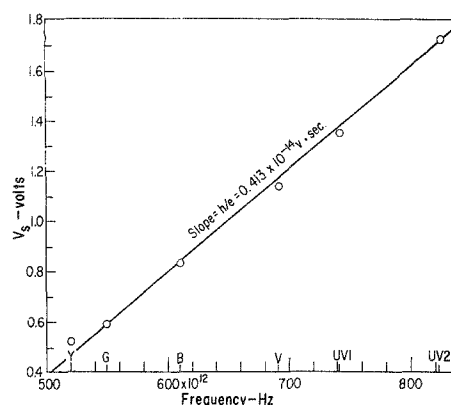


Fig. 1. Stopping potentials  $V_s$  plotted against frequency. The following data are plotted:

|      | $\lambda$ (Å) | $\nu$ (Hz)           | $V_s$ (V) |
|------|---------------|----------------------|-----------|
| uv 2 | 3650          | $822 \times 10^{12}$ | 1.72      |
| uv 1 | 4047          | $741 \times 10^{12}$ | 1.35      |
| V    | 4339          | $691 \times 10^{12}$ | 1.14      |
| B    | 4916          | $610 \times 10^{12}$ | 0.83      |
| G    | 5461          | $549 \times 10^{12}$ | 0.59      |
| Y    | 5770          | $520 \times 10^{12}$ | 0.52      |

ends of the cathode are rolled over its supporting wires so that its inner surface extends around to the outside, which is probably responsible for this rise. The optimum adjustment should give the largest cathode current with no detectable anode current. Calibration indicates that the least detectable anode current would be about 1/250 of the cathode current maximum. The value of retarding potential for apparent current cutoff is highest with the cell in this position, and is a helpful index of a suitable setting. It increases typically from about 1.6 V up to 2.4 V for a threshold output of 2  $\mu$ A at maximum gain as the ratio of anode to cathode current is reduced by orienting the cell. It has been possible in this way to adjust all of the 14 photocells purchased for this experiment from three different manufacturers. A removable handle clamped to the lower end of the photocell base facilitates this adjustment. Although the cells are less sensitive in this position, full scale output at the peak of the yellow line can yet be obtained with the gain available and a moderate slit opening.

## DETERMINATION OF THE STOPPING POTENTIAL

Curve A of Fig. 3 is the amplified and rectified photocurrent for the uv 2 line (3650 Å) plotted

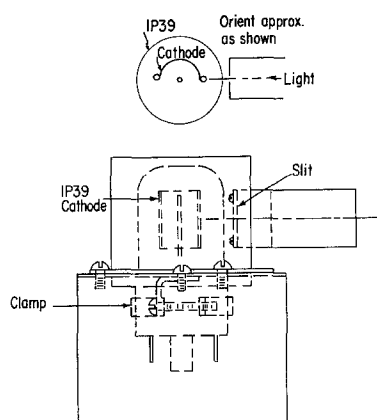


FIG. 2. Photocell mounting and orientation. The cell may be turned about its major axis until one edge of the cathode shadows the anode. The ratio of anode to cathode emission is greatly reduced in this position.

against potential. The point of inflection between retardation and the onset of saturation—about  $+0.4$  anode V or so—is usually taken as the actual zero of potential,<sup>6</sup> indicating that the contact difference of potential is in the retarding direction and is equal and opposite to the externally applied potential at this point. The actual retarding potential is the algebraic sum of these two potentials. Because of the curved foot and consequent offset of the rectifier characteristic curve C,  $12 \mu\text{A}$  must be added to the current values of curve A, giving curve A', which is proportional to the original photocurrent. Curve A' has been extended downward beyond the limit of curve A by increasing the gain to return the output current from 10 to  $100 \mu\text{A}$ , and by multiplying the new current readings by  $(10+12)/(100+12)$ . This was continued for a third range by again applying this procedure and multiplying by  $(22/112)^2$ . As the compensated photocurrent A' approaches zero it does not intersect the axis sharply, so that it is impracticable to determine  $V_s$  at the photocurrent cutoff. In fact the current only gradually falls to zero, where it remains, showing no indication of anode current even up to a retarding potential of 6 V, provided the tube has been oriented successfully. It happens that the square root of the compensated photocurrent is nearly linear with increasing negative applied potential in the main portion of its descent (Fig. 3, curve B). A straight line fitted to it and extended to the applied potential axis yields an

intercept which is taken as  $V_s$ .<sup>7,8</sup> In this way,  $V_s$  is determined by the portion of the curve in which the cathode current is much larger than any remaining anode current, or other residual current. Because the slopes of these curves differ for different wavelengths and gain settings, such a square root curve must be run for each wavelength (Fig. 4). This square root relationship between the lower portion of the photocurrent curve and the retarding potential was observed experimentally by Lukirsky and Prilezaev.<sup>7</sup> Wright<sup>8</sup> found that it held down to 1% of the saturation current and made use of it in determining the stopping potentials in an undergraduate laboratory experiment.<sup>9</sup> Especially constructed photocells were used in both of these experiments. They were designed with anodes surrounding the cathodes, so that all electrons could be collected by the anode. Although there seems to be no theoretical basis for it, Wright<sup>8</sup> justified its arbitrary use as (1) a uniform method of treating the data and (2) a practical way of extrapolating a curved line. The electrode geometry of the 1P39 is hardly favorable for this, and it is perhaps surprising that the relationship holds at all. But the square root current curve B is straight down to about  $3.5 (\mu\text{A})^{1/2}$ , so that it holds at least this far. This requires a rather long extrapolation of curve B, but the values of  $V_s$  seem to be reliable provided the extrapolation is

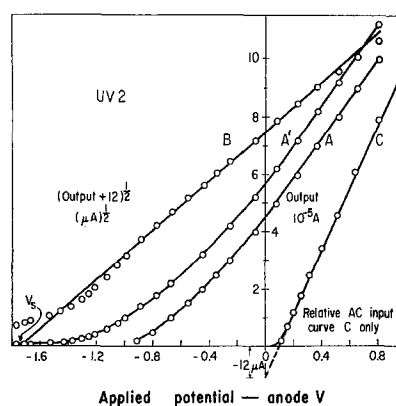


FIG. 3. Output current A and compensated output current A' plotted against applied potential. The rectifier characteristic C shows the compensation necessary to make A' proportional to the photocurrent. Curve B is the square root of A'. The intercept of the straight portion of B extended to the applied potential axis is taken as the stopping potential  $V_s$ .



spread between values obtained for  $h/e$ , careful experimenters obtained values within  $\pm 5\%$  of the accepted value, limited primarily by the accuracy of the voltmeter which measured  $V_s$ . Some students seemed to perform the experiment without understanding its full significance. It is important that the student be reminded that he is measuring electron energy and is observing directly its dependence upon the frequency of the ejecting photons.

# ACKNOWLEDGMENT

Scott Smith prepared the electronic layout and assembled and wired the circuits, and Herbert Scheibel photoetched the circuit boards and silk screened the labels on the amplifier-control units. Without this skilled collaboration, the construc-

tion of 12 of these units would have been much more difficult.

\* Present address: Army Electronics Command, Fort Monmouth, New Jersey.

<sup>1</sup> R. A. Millikan, Phys. Rev. **7**, 355 (1916).

<sup>2</sup> S. P. Davis, Amer. J. Phys. **29**, 707 (1961).

<sup>3</sup> A. Ahlgren, Phys. Teacher **1**, 183 (1963).

<sup>4</sup> H. H. Gottlieb, Phys. Teacher **3**, 343 (1965).

<sup>5</sup> R. J. Hanson and B. E. Clotfelter, Amer. J. Phys. **34**, 75 (1966).

<sup>6</sup> G. P. Harnwell and J. J. Livingood, *Experimental Atomic Physics* (McGraw-Hill, New York, 1933), pp. 214-219.

<sup>7</sup> P. Lukirsky and S. Prilezaev, Z. Physik **49**, 236 (1928).

<sup>8</sup> W. R. Wright, Amer. Phys. Teacher **5**, 65 (1937).

<sup>9</sup> M. Iona, Amer. J. Phys. **34**, 707 (1966). We were led to Refs. 7 and 8 by Iona's comment.

## Mechanical Models for Reactions Involving Isobaric Analog and Doorway States\*

P. A. MELLO

M. MOSHINSKY

*Instituto de Física*

*Universidad de México*

*México, D. F.*

(Received 20 February 1970; revised 11 May 1970)

*In this paper, we develop a classical mechanical model for nuclear reactions involving isobaric analog and doorway states. The R matrix for the model is identical to the one of the nuclear reaction problem, and the corresponding S matrix gives rise to such characteristic effects as the Robson enhancement factor for the isobaric resonances.*

# 1. INTRODUCTION

In the initial stages in the development of nuclear reaction theory, considerable use was made of mechanical, electric circuit, wave guide, etc., models to illustrate the concepts that were being introduced which eventually led to the

R- and S-matrix theory. Once the fundamental ideas became clear, the scaffolding provided by the models was abandoned, and when new concepts were required, they were formulated directly in the R- and S-matrix formalism.

While this procedure works fine with the experts in the field, it is not particularly transparent for those physicists that would like to follow the new ideas in nuclear reaction theory without mastering the detailed formalism. It is with these physicists in mind that we thought of models for such new concepts in nuclear reaction theory as isobaric analog and doorway states. While the models could be developed in a variety of branches of classical physics, we preferred mechanical models, as they employ the most familiar concepts.

We begin by discussing qualitatively the R- and S-matrix theory and its extensions to nuclear reactions involving isobaric analog states. This will suggest the main features of the mechanical model we require.

Soon after the experimental observation of narrow resonances in the cross section of low energy neutrons incident on nuclei, Bohr<sup>1</sup> proposed the idea of the compound nucleus mecha-